8th International Symposium on Magnetic Bearing
August 26-28, 2002, Mito, Japan

DEVELOPMENT OF LORENTZ FORCE TYPE SELF-BEARING MOTOR

Takahito Tokumoto
Dept. of Mechanical Eng., Ibaraki University, Hitachi, Ibaraki-Pref., 316-8511 Japan
ttokumo@mech.ibaraki.ac.jp

Daniel Timms
Dept. of Mechanical, Manufacturing and Medical Eng., QUT, Brisbane, Queensland, Q4001 Australia
d.timms@qut.edu.au

Hideki Kanebako, Ken-ichi Matsuda and Yohji Okada
Dept. of Mechanical Eng., Ibaraki University, Hitachi, Ibaraki-Pref., 316-8511 Japan
okada@mech.ibaraki.ac.jp

ABSTRACT

This paper introduces two self-bearing motors based on Lorentz force principles. A six-concentrated winding coil stator drives and levitates a rotor surfaced by eight strong permanent magnet (PM) poles. It therefore has merits of good dynamic response, good linearity and high reliability. The fundamental principle of rotational torque and radial force production is initially described, followed by the comparison of slot type and slotless type fundamental characteristics. An experimental rig is ultimately fabricated to practically confirm the proposed motor characteristics. These results enable the motors to be categorized into their respective applications.

INTRODUCTION

Recently, high speed and maintenance free motors are requested for high quality and high productivity machines. Due to their non-contact support, magnetic bearings have been gradually introduced into these machines[1]. However, initial magnetic bearing systems require a separate driving motor, leading to low bending vibrations caused by a relatively long shaft.

To overcome this problem, a self-bearing motor is developed which has combined functions of a radial magnetic bearing and AC motor[2][3][4].

In previously proposed PM type self-bearing motors, the levitation force is produced by reluctance force principle. However, this type is characterized by low efficiency and poor reliability. Non-linearity of the magnetic material also causes undesirable coupling between the two radial directions. Finally the surface permanent magnets must be thin, resulting in high cost, weak rotor strength and demagnetization problems in long-term use[5].

This paper introduces a new type of self-bearing motor based on Lorentz force principle. The rotor is surfaced by eight strong permanent magnets. The stator has two sets of six concentrated windings; one set supplies rotary torque whilst the other generates bearing forces. The rotor employs thick permanent magnets allowing for easier manufacturing, reduced demagnetization and good dynamic properties.

Two variations of the Lorentz type self-bearing motor were developed and are presented in this paper: The slotless type and the slotted type. Both are tested and their characteristics are compared.

THEORETICAL CONSIDERATIONS

The fundamental principles of this motor-bearing are initially introduced, followed by the theoretical development of rotation and levitation control independency.

Principle of Rotation

Figure 1 depicts the cross section of the cylindrical motor and one pair of motor coils.

The permanent magnets on the rotor produce the eight-pole strong magnetic flux in the air gap. The coils are wound inside the stator as shown in figure 1. The arrows in the figure indicate the directions of Lorentz force generation. Since the coils are fixed to the stator, a reaction torque is produced on the rotor, as described by the motoring toque arrow in the figure.

Principle of Levitation

The levitation coils are wound as oriented in the same place as the motor coils, as shown in Fig. 2.

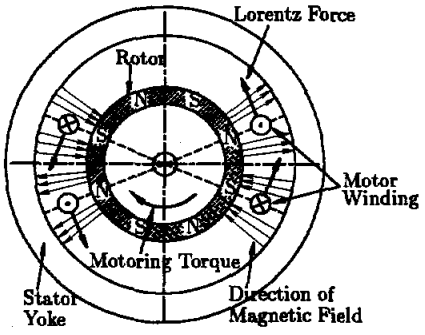

FIGURE 1: Principle of Giving Rotary Torque

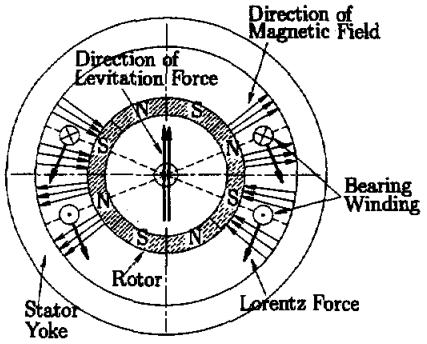

FIGURE 2: Principle of Giving Bearing Force

However, the current direction is inversed in the opposing coils, resulting in Lorentz forces acting similarly to cause the rotor to encounter radial forces. Six coils arranged around the stator can control the direction of radial force arbitrary.

Theoretical Analysis

The expanded schematic drawings of the slot type and the slotless type in the circumferential direction are shown in upper and lower parts of Fig. 3 respectively. The motoring and levitation coils are installed in the same positions inside the stator core. The entry and return paths of each coil are $\frac{\pi}{4}$ apart, corresponding to the width of the permanent magnets, to produce the maximum force. The U, V, W coils in the slotless type are placed $\frac{\pi}{3}$ apart. The slot ditches in the slotted type are also designed in the same position since the magnetic flux changes stepwise at this ditch. This has the same effect as the concentrated coil of the slotless type.

Suppose the following sinusoidal form approximates the airgap flux produced by the rotor Permanent Magnets.

$$B_g = -B\sin(\omega t + 4\theta) \tag{1}$$

Where the variables are defined in Table 1.

Rotational control The motoring coils are driven by the three phase currents,

TABLE 1: Definition of Variables

A	Magnitude of Motoring Current
B	Flux Magnitude by Permanent Magnet
C	Magnitude of Levitation Current
l	Effective Length of Windings
r	Diameter of Rotor
t	Time
ψ	Phase of Motoring Current
ϕ	Phase of Levitation Current
ω	Electric Frequency

$$\begin{aligned} I_{U_m} &= A\cos(\omega t + \psi) \\ I_{V_m} &= A\cos(\omega t + \frac{2}{3}\pi + \psi) \\ I_{W_m} &= A\cos(\omega t + \frac{4}{3}\pi + \psi) \end{aligned} \tag{2}$$

From Eq. (2) the current distribution in the circumferential direction is written by Dirac's delta function. The torque produced can then be calculated as the following [5],

$$T = 2rl_m \int_{-\frac{\pi}{8}}^{\frac{7}{8}\pi} B_g i_1 d\theta = 6rl_m AB\cos\psi \tag{3}$$

The torque can be controlled by the current magnitude A and phase ψ in Eq. (3), and it is independent from rotor position and time.

Levitation control The levitation coils are driven by the three phase currents,

$$\begin{aligned} I_{U_b} &= C\cos(\omega t + \phi) \\ I_{V_b} &= C\cos(\omega t + \frac{2}{3}\pi + \phi) \\ I_{W_b} &= C\cos(\omega t + \frac{4}{3}\pi + \phi) \end{aligned} \tag{4}$$

From Eq. (4) the levitation force can be calculated as follows [5],

[y directional force]

$$F_y = l_b \int_{-\frac{1}{8}\pi}^{\frac{15}{8}\pi} B_g i_2 \cos\theta d\theta = \frac{3\sqrt{2+\sqrt{2}}}{2} Bl_b C\cos\phi \tag{5}$$

[x directional force]

$$F_x = l_b \int_{-\frac{1}{8}\pi}^{\frac{15}{8}\pi} B_g i_2 \sin\theta d\theta = -\frac{3\sqrt{2+\sqrt{2}}}{2} Bl_b C\sin\phi \tag{6}$$

From Eqns. (5) and (6) the levitation is independently controlled from the rotation. The levitation force can be controlled only by the current magnitude C and phase angle ϕ.

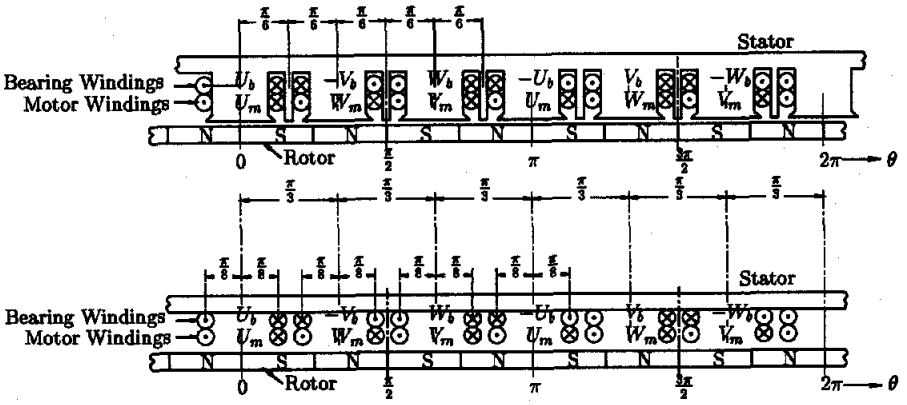

FIGURE 3: Arrangement of Motor and Bearing Windings (Slotless and Slot-Type)

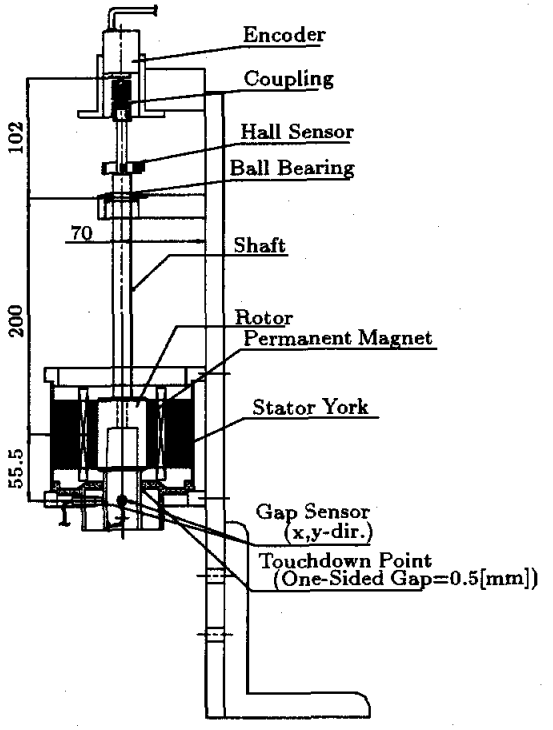

FIGURE 4: Schematic of Experimental Setup

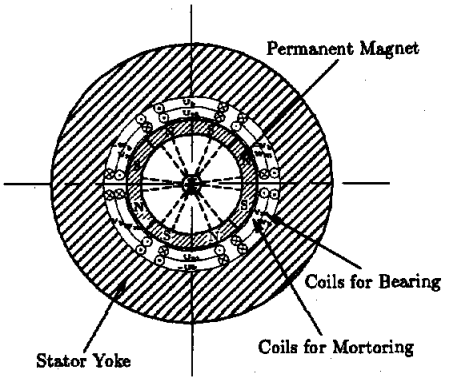

FIGURE 5: Arrangement of Coils

TABLE 2: Control Parameters

	Slotless	Slot	Unit
K_p	15	10	[A/mm]
K_d	0.04	0.015	[A · sec/mm]
K_i	8	8	[A/(sec · mm)]
τ	0.1	0.1	[msec]
T_d	0.8	0.8	[msec]

EXPERIMENTAL SETUP

The experimental setups are constructed to confirm the proposed theory and compare their properties. The general schematic is shown in figure 4. The motor is a cylindrical, vertically set inner rotor type. A ball bearing is installed 200[mm] above the motor to support the x, y and z directions. Hence the rotor has two degrees of freedom in the x and y directions. Two gap sensors are installed below the motor to detect x and y directional displacements, while the encoder and the Hall sensor are installed above the rotor to detect angular position.

The experiment is performed using the slotless type and slot type self-bearing motors.

Schematic of Stator

Both the motoring and levitation coils of the slotless type are glued in the same circumferential position inside the rotor as shown in Fig. 5. In the slot type, the flux changes stepwise at the ditch, therefore the ditches of the stator are also designed at these positions. This allows the equations (5) and (6) to hold true for levitation force generation. For this purpose main slots and sub slots are used, as shown in Fig 6. The motoring coils are arranged by U_m, V_m, W_m 120° apart with the opposite coils connected in phase, whilst the levitation coils are arranged by U_b, W_b, V_b in the same positions with the opposite coils connected out of phase.

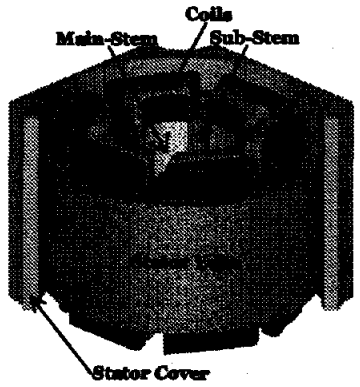

FIGURE 6: Schematic of stator (Slot-Type)

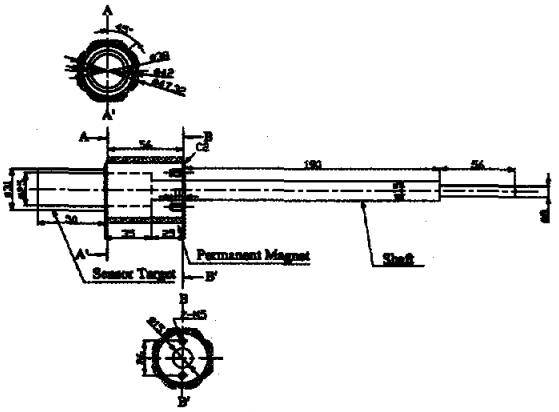

FIGURE 8: Schematic of Rotor (Slot-Type)

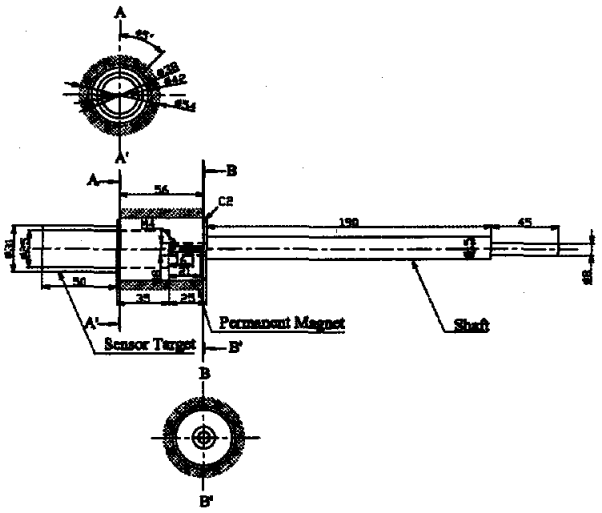

FIGURE 7: Schematic of Rotor (Slotless-Type)

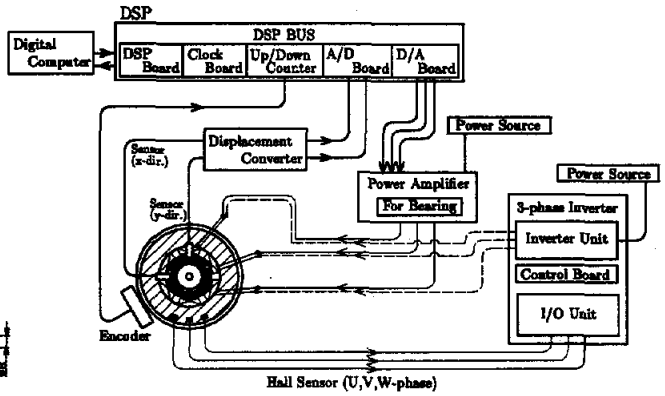

FIGURE 9: Schematic of Control System

Schematic of Rotor

The schematic of the slotless rotor is shown in Fig. 7, whilst Fig. 8 displays the slot type. The shaft design incorporates enough high bending mode so as not to affect levitation control. The permanent magnets in the slot type were designed using FEM magnetic field analysis, resulting in a semi-cylindrical shape to reduce cogging torque. Eight Neodymium permanent magnets were glued with alternating poles around the circumference of the rotor in both cases.

Control System

A schematic of the control system is shown in Fig 9. Levitation is controlled via a digital signal processor (DSP). Measured radial displacements are input into the DSP via A/D converters. A control algorithm, based on the digital PID controller, calculates the required levitation current of each phase windings according to the measured rotor angular displacement. D/A converters output these currents to APEX PA-12 power amplifiers that have a supply voltage of ±24[V].

A three phase PWM inverter is used for rotation control. The speed demand signal is input into the computer, and each of the coil currents are calculated according to the rotor angle before being output into the Y connected motor coils. The motoring and levitation currents are independent of each other.

The levitation control parameters are listed in Table 2, where K_p is the proportional gain, K_d is the derivative gain, K_i the integral gain, T_d the derivative time constant and τ is the sampling time interval.

EXPERIMENTAL RESULTS AND CONSIDERATIONS

Levitation and levitated rotating tests are carried out for both slot and slotless types.

Force and Torque

Figures 10 and 11 present the measured values of force and torque, with the dotted lines representing the theoretical values calculated from eqns. (3) and (6). The linear levitation forces shown in Fig. 10

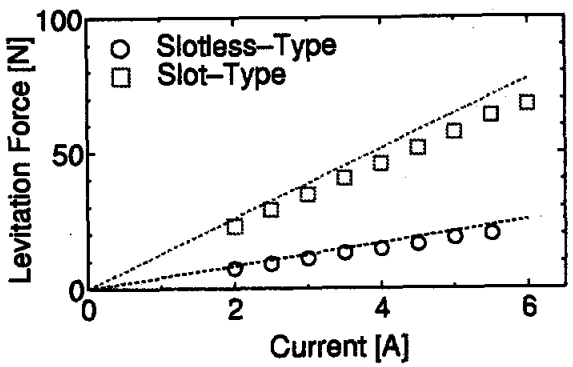

FIGURE 10: Levitation Force

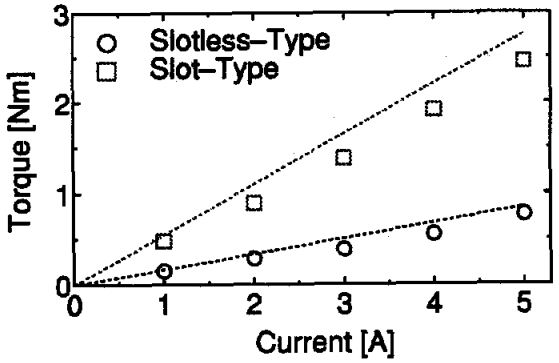

FIGURE 11: Static Torque

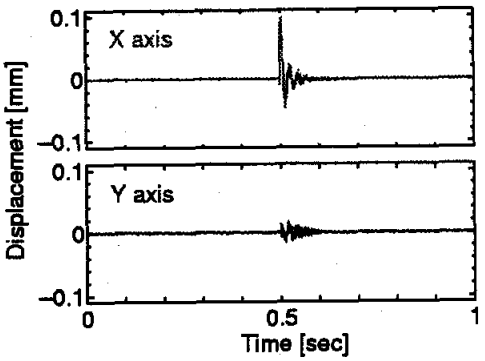

FIGURE 12: Impulse Response for x-axis (Slotless-Type)

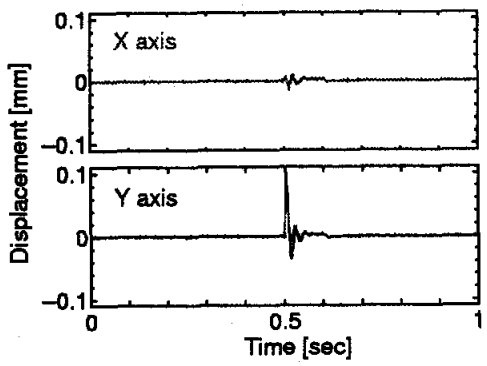

FIGURE 13: Impulse Response for y-axis (Slotless-Type)

result in a maximum levitation force production of 14[N] and 46[N] for slotless and slot types respectively, recorded at a levitation current of 4[A].

The linear torque property was also measured and displayed in Fig. 11. Torque constants of 0.17 [Nm/A] for slotless and 0.49[Nm/A] for slot type were recorded.

Relatively good linearity and strong characteristics are obtained from the torque and levitation force measurements, with the slot type producing forces approximately three times greater than those produced in the slotless arrangement. These results confirm the purpose of achieving a strong slot type self-bearing motor.

Impulse Response

Impulse response is measured to confirm levitation stability. The rotor was hammered and the decaying response was recorded and displayed in Figs. 12 to 15. Figures 12 and 14 describe the response in the x direction whereas Figs. 13 and 15 describe the y direction response. All the transient responses decay within 0.1[sec]. However, the responses of the slot type indicate poor damping, which is considered as a slower dynamic response due to high coil inductance.

Independent vibration between the x and y directions is almost recognized from these measured data, although some influence is seen when the hammering direction is not entirely in line with the measured axis.

Levitated Rotation

Rotating the levitated motor and recording the steady state vibration measured the unbalance responses. The results are shown in Fig. 16.

The highest vibration of slotless type is recorded at 2400[rpm], which is considered to be the influence of the rigid mode. Above this peak, the vibration is decreased and the rotor runs at the center of inertia. The top speed is restricted to 5500[rpm] to avoid the centrifugal tear off of the permanent magnets, and can thus be improved by redesign.

The slot type motor can run up to 2100[rpm]. Near this top speed however, the levitation voltage approaches the supply voltage and the levitation becomes unstable. This is considered to be the result of the high inductance of the slotted coil leading to high Back-Electromotive-Voltage.

Motor Efficiency

To confirm the motors capability, the input to output power ratio is measured and shown in Fig. 17 to characterize the motor efficiencies.

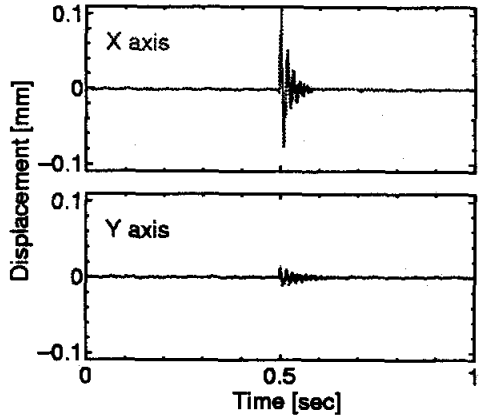

FIGURE 14: Impulse Response for x-axis (Slot-Type)

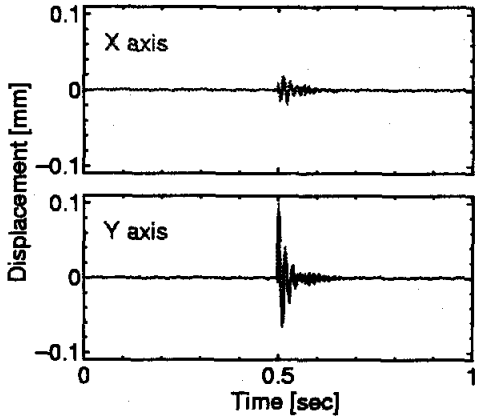

FIGURE 15: Impulse Response for y-axis (Slot-Type)

The maximum efficiency for the slotless type motor was 89[%] whilst the slot type motor recorded a maximum of 58[%]. These measurements were conducted with a supply voltage of 80[V] to the inverter.

High efficiency may be realized by the slot type motor due to low leakage flux loss. However, the lower efficiency encountered is mainly attributed to a combination of core losses and cogging torque loss, both considered as main drawbacks of the slot type self-bearing motor.

CONCLUSIONS

Lorentz force type self-bearing motor is proposed which can be applicable to the 8 pole motor with 6 concentrated coils. Analytical results confirmed that the rotation and levitation can be controlled independently.

Two types of experimental setup are made and tested. The slotless motor can run up to 5500[rpm] with stable levitation. However the slot type can run up to 2100[rpm] and the motor efficiency is 58[%]

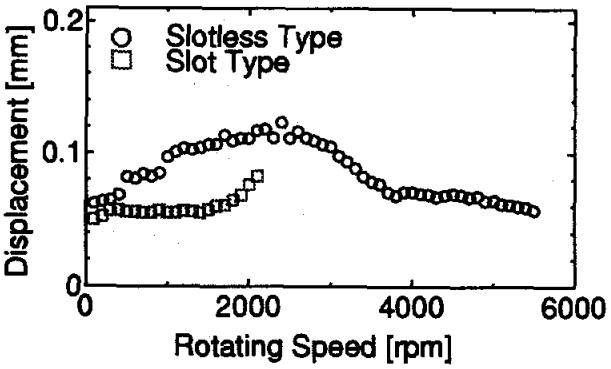

FIGURE 16: Unbalance Response

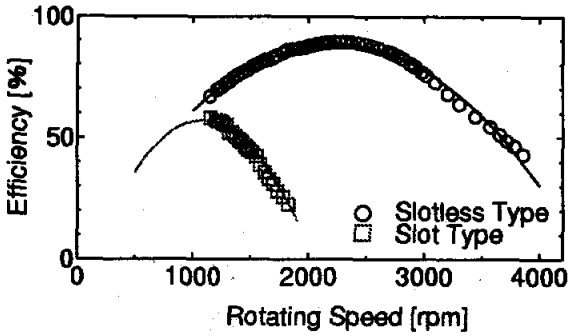

FIGURE 17: Motor Efficiency

which is lower than the slotless type.

However the slot type showed about three times strong rotation and levitation. Hence the slotless type is adequate for high efficient, low torque and high speed application, while the slot type is adequate for high torque, low speed application. Further work is continuing to develop a new construction which will have better performance and to apply to the real machines such as artificial heart and hard disc drive.

References

1. Okada, Y., et. al., Fundamental and Application of Magnetic Bearings, JSME, Yokendo, 1995 (in Japanese)
2. Okada, Y. et. al., IEEE Trans. on Industry Applications, Vol. 31, No. 5, 1995, pp. 1047-1053
3. A. Chiba, et al. : IEEE Trans. on Energy Conversion, Vol. 9, No. 1, 1994, pp. 61-67
4. R. Schöb and N. Barletta : Proc. of 5th Int. Symp. on Magnetic Bearings, Kanazawa, Japan, 1996, pp. 313-318
5. Okada, Y. et. al., Lorentz Force Type Self-Bearing Motor, Proc. of 7th Int. Symp. on Magnetic Bearings, ETH Zurich, August 23-25, 2000, pp. 353-358